Published in final edited form as:
Exp Cell Res. 2013 August 1; 319(13): 2113–2123. doi:10.1016/j.yexcr.2013.05.005.

Retinal Pigment Epithelium (RPE) exosomes contain signaling phosphoproteins affected by oxidative stress

Lucia Biasutto[a,b,*], **Antonella Chiechi**[c], **Robin Couch**[d], **Lance A. Liotta**[c], and **Virginia Espina**[c,*]

[a]CNR Institute of Neuroscience, Viale G. Colombo 3, 35121 Padova, Italy

[b]Department of Biomedical Sciences, University of Padova, Viale G. Colombo 3, 35121 Padova, Italy

[c]Center for Applied Proteomics and Molecular Medicine, George Mason University, 10900 University Blvd, Manassas, VA 20110, USA

[d]Department of Chemistry and Biochemistry, George Mason University, 10900 University Blvd, Manassas, VA 20110, USA

Abstract

Age-related macular degeneration (AMD) is a leading cause of vision loss and blindness among the elderly population in the industrialized world. One of the typical features of this pathology is the gradual death of retinal pigment epithelial (RPE) cells, which are essential for maintaining photoreceptor functions and survival. The etiology is multifactorial, and oxidative stress is clearly one of the key factors involved in disease pathogenesis.

Recent work has revealed the presence of phosphorylated signaling proteins in the vitreous humour of patients affected by AMD or other retinal diseases. While the location of these signaling proteins is typically the cell membrane or intracellular compartments, vitreous samples were proven to be cell-free.

To gain a better understanding of how these proteins can be shed into the vitreous, we used Reverse Phase Protein Arrays (RPMA) to analyze the protein and phosphoprotein content of exosomes shed by cultured ARPE-19 cells under oxidative stress conditions.

72 proteins were shown to be released by ARPE-19 cells and compartmentalized within exosomes. 41 of them were selectively detected in their post-translationally modified form (i.e., phosphorylated or cleaved) for the first time in exosomes. Sets of these proteins were linked together reflecting activation of pathway units within exosomes. A subset of (phospho)proteins were altered in exosomes secreted by ARPE-19 cells subjected to oxidative stress, compared to that secreted by control/non stressed cells. Stress-altered exosome proteins were found to be involved in pathways regulating apoptosis/survival (i.e, Bak, Smac/Diablo, PDK1 (S241), Akt (T308), Src (Y416), Elk1 (S383), ERK 1/2 (T202/Y204)) and cell metabolism (i.e., AMPK α1 (S485), Acetyl-CoA carboxylase (S79), LDHA).

[*]*Corresponding authors:* Lucia Biasutto: CNR Institute of Neuroscience, c/o Dept. Biomedical Sciences, Viale G. Colombo, 3, 35121 Padova, Italy. Fax: +39 0498276049. Phone: +390498276483. lucia.biasutto@cnr.it.; Virginia Espina: Center for Applied Proteomics and Molecular Medicine, George Mason University, 10900 University Blvd, MS 1A9, Manassas, VA 20110, USA. Fax: 1-703-993-8606. Phone: 1-703-993-8062. vespina@gmu.edu..

Exosomes may thus represent the conduit through which membrane and intracellular signaling proteins are released into the vitreous. Changes in their (phospho)protein content upon stress conditions suggest their possible role in mediating cell-cell signaling during physio-pathological events; furthermore, exosomes may represent a potential source of biomarkers.

Keywords

ARPE-19 cells; exosomes; Reverse Phase Protein Arrays; Age Related Macular Degeneration; Oxidative stress

Introduction

Retinal age-related macular degeneration (AMD) is the leading cause of vision loss and blindness in individuals over age 60 in the industrialized world (Gehrs et al, 2006). The typical features of AMD include accumulation of extracellular deposits (drusen) in the macula, thickening of Bruch's membrane, and gradual death of retinal pigment epithelial (RPE) cells and photoreceptors. As RPE cells and photoreceptors degenerate, there is a tendency for blood vessels to grow from their normal location in the choroid into an abnormal location beneath the retina. The abnormal blood vessels are dysfunctional and leaky, resulting eventually in progressive and severe loss of central vision.

Initial pathogenesis of AMD involves the degeneration of RPE cells, which progressively causes the death of rods and cones. RPE cells are essential for maintaining photoreceptor functions and survival: they are involved in the absorption of light energy, transport of metabolites and nutrients between photoreceptors and choriocapillaries, expression of growth factors for photoreceptors, and are responsible for phagocytizing shed photoreceptor outer segments, regulating the visual cycle and creating the blood-retinal barrier (Boulton and Dayhaw-Barker 2001; Kevany and Palczewski 2010).

The aetiology of AMD is multifactorial, including genetic, environmental, nutritional and behavioural factors (Ding et al, 2009; Zarbin, 2004; Kaarniranta and Salminen 2009; Jager et al, 2008); oxidative stress is clearly involved in the pathogenesis (Plafker, 2010; Qin, 2007). The retina is the tissue with the highest metabolic rate in the body (Yu and Cringle, 2001), and high oxygen consumption usually is accompanied by Reactive Oxygen Species (ROS) generation. RPE cells generate ROS due to phagocytosis of photoreceptor outer segments (Miceli et al, 1994), which also determines progressive accumulation of lipofuscin (Dorey et al, 1989), a mixture of non-degradable protein-lipid aggregates that leads to ROS generation upon irradiation with light (Wu et al, 2010; Wolf, 2003; Ng et al, 2008). Treatment with antioxidants reduces the progression of the pathology (Johnson, 2010). Inflammation is also linked to oxidative stress (Tschopp, 2011), and has an important role in AMD pathogenesis (Kaarniranta and Salminen, 2009).

Proteomic analysis of vitreous samples coming from patients affected by AMD or other retinal diseases and undergoing anti-VEGF therapy reported the presence of phosphorylated receptors and signaling proteins in the vitreous (Davuluri et al, 2009; Tamburro et al, 2010). Activated growth factor receptors had not been previously described in the vitreous; the relative abundance of certain proteins was dependent on the underlying retinal disease, and on whether patients were responders or non-responders to anti-VEGF therapy. These findings may thus constitute the basis of a new class of biomarkers for diagnosis and individualized therapy. These receptors normally reside in the cellular membrane, but the vitreous fluids in which they were identified were proven to be clear and cell-free. These

findings raised the question of whether or not vitreous phosphoproteins or even portions of entire signal pathways were encapsulated within exosomes or microvesicles.

Increasing evidence points to exosomes and microvesicles as a novel alternative mechanism for protein export and intercellular communication, permitting exchange of proteins, lipids and nucleic acids between cells (Février and Raposo, 2004; Belting and Wittrup, 2008; Ahmed and Xiang, 2011). Exosomes are 40-100 nm membrane vesicles of endocytic origins. They form intracellularly by inward budding of the membrane of endosomes, leading to multivesicular bodies (MVBs); MVBs eventually fuse with the plasma membrane, releasing their internal vesicles (i.e., exosomes) in the extracellular medium. Exosomes from different cellular origins contain a common set of molecules (which are essential for their biogenesis, structure and trafficking), as well as cell type-specific components. They are secreted by most cell types *in vitro*, and found also *in vivo* in different body fluids (blood, urine, saliva, etc.) (Simpson et al, 2008; van Niel et al, 2006).

To gain a better understanding of how phosphoproteins can be shed into the vitreous, we used Reverse Phase Protein Arrays (RPMA) (Charboneau et al, 2002; Wilson et al, 2010) to analyze the protein and phosphoprotein content of exosomes shed by cultured ARPE-19 cells (a non transformed human RPE cell line) exposed to oxidative stress conditions.

Materials and methods

ARPE-19 cells culture

ARPE-19 cells (a non-transformed human RPE cell line) were obtained from American Type Culture Collection (ATCC, Manassas, VA). ARPE-19 cells were cultured in DMEM: F12 medium (ATCC) supplemented with 10% fetal bovine serum (FBS; from ATCC), at 37°C in a humidified 5.0 % CO_2 atmosphere.

Preparation of exosome-production medium

The culture medium used for preparing cell-conditioned media, from which exosomes were isolated, was depleted of contaminating FBS-derived exosomes according to the procedure described previously (Théry et al, 2006). Briefly, culture medium containing 20% FBS was centrifuged overnight (16 h) at 100,000*g*, 4°C. The supernatant was filter-sterilized and diluted with culture medium without FBS to 10% final FBS.

ARPE-19 viability assay

ARPE-19 cells were seeded at a density of 11,000 cells/cm^2 onto 96-well plates. 3 days after seeding, cells were incubated for 24 h with exosome-production medium containing different concentrations of Rotenone (0 - 5 μM; Sigma) or Methyl Viologen (0 - 2000 μM; ACROS Organics). At the end of the treatments, cell viability was quantified by CellTiter-Blue™ assay (Promega), adding 20 μl/well of Resazurin dye solution and incubating in the dark at 37°C for 2 h. Fluorescence was recorded using a Microplate Reader (Fluoroskan, Ascent FL Labsystems; excitation wavelength 530 nm, emission 584 nm). All assay points were determined in triplicate, and experiments were repeated three times.

ARPE-19 cell treatments

ARPE-19 cells were seeded onto T75 culture flasks at a density of 11,000 cells/cm^2, and grown three days until they reached confluency. After washing once with PBS and once with medium without FBS, cells were incubated 24 h in exosome-production medium with: - no further additions (control), or - 2.5 μM Rotenone, or - 62.5 μM Methyl Viologen. These concentrations were the maximum dose that did not affect cell viability, and thus were chosen to avoid the presence of contaminating apoptotic blebs in the final exosome

preparation (Théry et al, 2001). To isolate sufficient amounts of exosomes, about 17.5×10^6 cells were used for each treatment; experiments were repeated three times for each condition.

Following cell treatments, conditioned medium was collected and stored at 4°C until exosome isolation. An aliquot of the cells (about 2.5×10^6) was washed twice with cold PBS, and lysed with 1 ml of extraction buffer (a 10% solution of TCEP (Pierce) in T-PER™ 2× (Pierce)/ SDS Tris-glycine 2× buffer (Invitrogen)). Cell lysates were immediately heated 7 min at 100°C, and stored at −80°C prior to microarray construction. The remaining cells (about 15×10^6) were further incubated in exosome-production medium without any treatment/addition for another 96 h period; conditioned medium was then collected and stored at 4°C until exosome isolation, and cell lysates were prepared as described above.

Exosome isolation

Exosomes were isolated from conditioned media (60-70 ml from each treatment), according to the protocol described previously (Théry et al, 2006). Briefly, cell culture media were centrifuged at 4°C sequentially for 10 min at 300*g*, 20 min at 2,000*g*, and 30 min at 10,000*g*. After each centrifugation step, the pellet was removed and discarded. Exosomes were then precipitated by ultracentrifugation of the supernatant (70 min at 100,000*g*, Optima™ XL-80k Ultracentrifuge, Beckman, SW28 rotor), and washed by resuspending the pellet in PBS and centrifuging again for 70 min at 100,000*g*. Ultracentrifugation was performed using polyallomer tubes (Beckman).

Exosome lysates were prepared by suspending the final pellet in 20 μl of extraction buffer, and immediately heating the pellet for 7 minutes at 100°C. Exosome lysates were stored at −80°C prior to microarray construction.

AFM analysis

Exosomes were characterized by Atomic Force Microscopy (AFM) using an NSCRIPTOR™ DPN® System (NanoInk). After exosome isolation (see above), the pellet was resuspended in 50 μl PBS, deposited on freshly cleaved mica under humid atmosphere at room temperature for 15 minutes, and dried under nitrogen before measurement. Images were acquired in the AC mode using a silicon tip with a typical resonance frequency of 300 kHz and a radius smaller than 10 nm.

RPMA construction

Cell and exosome lysates were printed undiluted on a glass-backed nitrocellulose array slide (20 × 50 mm; Schott) using an Aushon 2470 robotic arrayer (Aushon BioSystems) equipped with 350 μm pins, as previously described (VanMeter et al, 2007; Speer et al, 2007). Albumin was used for protein concentration calibration; it was printed in triplicate on the same slide, in eight-point dilution curves (0.08 - 1 mg/ml). Total protein concentration values per microarray spot was determined with Sypro Ruby protein stain (Invitrogen) per manufacturer's directions, and imaged with a CCD camera (NovaRay; Alpha Innotech). The protein content of each sample was estimated by comparison to the albumin calibration curve. Lysates were then diluted appropriately to obtain a sample concentration of 0.5 mg/ml total protein in the neat spot, and printed on nitrocellulose array slides (Schott). Each sample was printed in duplicate; cell lysates were printed in a 4 point dilution curve (Fig. 1), while exosomes were printed only as neat sample. Cellular lysates prepared from Hela ± pervanadate, Hela + Heat Shock, A431 ± EGF, HepG2, T98G, Mouse Macrophage + LPS/ IFNγ and MCF-7 were printed on each array for quality control assessments of (phospho)protein loading and detection. Slides were stored with desiccant (Drierite; WA Hammond) at −20°C prior to immunostaining.

RPMA detection

Immunostaining was performed on an automated slide stainer per manufacturer's instructions (Autostainer CSA kit; Dako), as previously described (VanMeter et al, 2007; Speer et al, 2007). Each slide was incubated with a single primary antibody at room temperature for 30 min. The full list of primary antibodies used is reported in Supplementary Table 1. Antibodies were previously validated by Western Blot to ensure they give a single (> 80% total signal) specific band (VanMeter et al, 2008). The negative control slide was incubated with antibody diluent instead of antibody. Secondary antibody was goat anti-rabbit IgG H+L (1:10,000) (Vector Labs), or goat anti-mouse IgG (1:25) (Dako). Subsequent signal detection was amplified via horseradish peroxidase mediated biotinyl tyramide deposition with chromogenic detection (Diaminobenzidine) per manufacturer's instructions (Dako) (Fig. 1).

Each array was scanned, and spot-intensity analyzed. Spot intensity was integrated over a fixed area; local area background intensity was determined for each spot from the unprinted adjacent slide background (Image Quant v5.2; GE Healthcare). Non-specific background staining of the secondary antibody was subtracted, and data was normalized per microarray spot, according to Chiechi et al, 2012; a standardized single data value was generated for each sample on the array. NormFinder software was used to find the optimal normalization protein (Andersen et al, 2004).

Statistics

Significance in comparisons between groups was assessed using the non parametric Wilcoxon Rank Test (Wilcoxon-Mann-Whitney test; GraphPad Prism 6 software). We considered this test as the most appropriate to compare small size samples, since it does not require any assumption about the normality of the data distribution for a small N number.

Results

RPMA - Data generation and normalization

RPMA (Wilson et al, 2010; VanMeter et al, 2007; Speer et al, 2007) were used to identify the signaling pathways affected by oxidative stress in ARPE-19 cells, an immortalized human cell line that is widely used as an RPE model *in vitro* (Dunn et al, 1996), and to characterize for the first time the (phospho)protein content of exosomes shed by these cells (Fig. 1).

Antibodies used for RPMA staining were previously validated through Western Blot for their specificity. Only antibodies which gave a single band (> 80% total signal) specific for the target protein (or its specific post-translationally modified form) were used.

NormFinder software was used to find the protein with the greater expression stability among samples, which was then used to normalize data (Chiechi et al, 2012; Andersen et al, 2004). This was found to be β-actin (if only cells were considered) or cd63 (if only exosomes were considered). Therefore β-actin and cd63 normalization were preferred to compare protein levels between cells or between exosomes, respectively.

We avoided normalization to total protein, since it has been reported that culture media serum proteins associate with microvesicles (Palmisano et al, 2012), and thus may cause overestimation of sample total protein levels.

Exosome isolation and characterization

Exosomes shed by ARPE-19 cells were isolated with a series of centrifugation and ultracentrifugation steps, according to a commonly used protocol (Théry et al, 2006; see Materials & Methods). They were then characterized through Atomic Force Microscopy (AFM) (Palanisamy et al, 2010; Sharma et al, 2010); images revealed that the vast majority of the samples consisted of small vesicles with 80-110 nm diameter (Fig. 2A). A few larger particles were also present, which might be exosome aggregates (which are known to be difficult to avoid after ultracentrifugation; Théry et al, 2006), or larger microvesicles.

Exosomes were further characterized through RPMA analysis by the presence of the exosomal protein markers cd63 and cd9 (Théry et al, 2002). Other proteins were present in exosomes at higher levels, compared to the corresponding cell lysates (Fig. 2B and Tab. 1). Among these are RPE-65 (a typical marker of RPE cells) and TLR3. Since TLR3 is present mostly in endosomal membranes (Barton and Kagan, 2009; Kawai and Akira, 2010), its abundance supports the endocytic origin of these vesicles, and thus their identification as exosomes.

To compare protein levels in cells *vs* exosomes, we normalized data to a third protein, LC3B. This was found to be the most stably expressed protein (Chiechi et al, 2012; Andersen et al, 2004) if cells and exosomes were considered together. LC3B is intended as the total LC3B pool, and not as the lipidated form LC3B II, which is a marker for autophagy. Furthermore, conclusions drawn normalizing data to LC3B were consistent with data obtained with β-actin or cd63 normalization.

ARPE-19 exosomes contain a novel set of signaling phosphoproteins

RPMA analysis of exosomes and corresponding cell lysates was performed over 75 endpoints representing key disease related pathways associated with autophagy, oxidative stress, cell adhesion, angiogenesis, and pro-survival/apoptotic pathways (Supplementary Table 1).

RPMA analysis of exosomes revealed 72 proteins. We consulted Exocarta, a compendium for proteins, RNA molecules and lipids identified in exosomes (Mathivanan ans Simpson, 2009; Mathivanan et al, 2012), and compared the proteins already present in the database (4563 proteins in February, 2013) with those found in exosomes during this study. 13 of the proteins analyzed here were detected in exosomes for the first time, and 41 were specifically detected in their phosphorylated or cleaved form for the first time. Table 1 reports the complete list of the proteins detected in exosomes during this study, their previous detection, and their relative abundance in exosomes compared to cells.

An intriguing aspect of these results was the detection of proteins in their phosphorylated state; since phosphorylation reflects the activation state of signaling pathways, phosphoprotein content may be critical for defining a role of exosomes in intercellular signaling. Compared to control, the levels of certain proteins were altered in exosomes shed by stressed ARPE-19 cells. Among these were phosphorylated members of pathways regulating survival, proliferation, apoptosis and cell metabolism (Tab. 2).

Oxidative stress modifies signaling protein content of ARPE-19 cells

Since oxidative stress plays a key role in AMD pathogenesis, and to take into account possible differences in cellular response to different agents (Weigel et al, 2002; Lu et al, 2006), ARPE-19 cells were treated with Methyl Viologen, a pro-oxidant that leads to superoxide radical generation (Suntres, 2002), or alternatively with Rotenone, a known inhibitor of mitochondrial Complex I. Inhibition of the respiratory chain leads to an

increased production of mitochondrial ROS, with consequent mitochondrial DNA damage and further ROS generation due to defective respiratory chain (Koopman et al, 2010); moreover, an increase in defective mitochondria can cause overloading of lysosomes in RPE cells, stimulation of autophagy, and further ROS production (Wang et al, 2009).

RPMA analysis of cell lysates exposed to Rotenone or Methyl Viologen showed altered levels of many (phospho)proteins involved in signaling pathways regulating apoptosis (i.e., cleaved caspases 3 and 9; Bad (S112)), proliferation and survival (i.e., cRaf (S338), Akt (T308), CREB (S133)), angiogenesis (i.e., PDGFRβ (Y716) and (Y751), VEGFR (Y951)), adhesion (i.e., FAK (Y576/577) and (Y397)), metabolism (i.e., GSK3 αβ (Y279/Y216), AcetylCoA carboxylase (S79)), inflammation (i.e., COX2, Stat3 (S727)) (Fig. 3). RPMA analysis did not detect cleaved PARP (an hallmark of apoptosis; Oliver FJ et al, 1998) in all ARPE-19 cell samples, while it was present in quality control cell lysates printed at similar concentrations in the same slide.

Some of the alterations observed in cell lysates exposed to oxidative stress reflect signaling perturbations observed during AMD (Fig. 4). For example, levels of autophagy associated Beclin-1 and Atg12 were increased; autophagy markers have been found in drusen of AMD patients, and stressed RPE cells have been reported to increase their autophagic activity (Wang et al, 2009).

Phosphorylated forms of FAK (FAK (Y576/577): Maa and Leu, 1998; FAK (Y397): Schlaepfer et al, 1999) were decreased. FAK is an important cell signaling mediator involved in cell migration, survival and cell cycle regulation; its phosphorylation was reported to be essential for RPE phagocytic activity, and it is decreased/compromised in age-related retinal diseases (Nandrot et al, 2004; Finnemann, 2003).

Discussion

It has been previously reported that RPE cells are able to secrete exosomes, and exosome markers have been found in drusen in eyes with AMD (Wang et al, 2009). However, to our knowledge this is the first extensive (phospho)proteomic characterization of RPE-secreted exosomes. A previous proteomic study was performed on RPE membrane blebs (Alcazar et al, 2009), but these are a different class of vesicles. Blebs are bigger than exosomes, originate directly from the plasma membrane and can be precipitated from conditioned medium through 15 min of a 100*g* centrifugation. Exosomes, on the other hand, have an endocytic origin, and can be precipitated only after 1 hour of a 100,000*g* ultracentrifugation of the medium (previously deprived of larger vesicles through sequential centrifugation steps at lower, increasing speeds).

RPMA technology is an optimal proteomic method for exosome analysis because it is quantitative, high throughput, multiplexed, high in sensitivity and can be applied to proteins from extremely small amounts of input material (Wilson et al, 2010; Mueller et al, 2010). RPMA is most often used for measuring post-translational modifications; the sensitivity of detection for the RPMAs is such that low-abundance phosphorylated protein isoforms can be measured from a spotted lysate representing fewer than 10 cell equivalents (VanMeter et al, 2008). Compared to Western Blot, ELISA, or traditional proteomic technologies such as two-dimensional gel electrophoresis, RPMA are thus particularly suitable for analysis of small sample amounts (i.e., biopsies or vitreous samples) and detection of low abundance post-translationally modified proteins in exosomes.

Exosomes have been extensively characterized for their protein, mRNA, miRNA and lipid content (see the ExoCarta Database) (Mathivanan and Simpson, 2009; Mathivanan et al, 2012); however, to our knowledge only 2 previous papers deal with post-translationally

modified proteins included in these vesicles (Gonzales et al, 2009: urinary exosomes; Palmisano et al, 2012: beta cell-derived microparticles and exosomes). Moreover, the present study quantitatively evaluated a comprehensive list of exosome phosphoproteins that are members of disease relevant signal pathways.

Several proteins and phosphoproteins have been detected in exosomes for the first time in this study. Among the 72 proteins detected in exosomes, 13 were not previously reported to be present in exosomes, and 41 were specifically detected for the first time in their post-translationally modified form (phosphorylated or cleaved). Some of them were the same phosphorylated receptors that were found in the vitreous of patients: PDGFRβ (Y751) and (Y716), VEGFR2 (Y996), c-kit (Y703) (Davuluri et al, 2009).

The relative abundance of the proteins detected in exosomes was often different from that in the corresponding cells. Importantly, in addition to the exosome markers cd9 and cd63, ARPE-19 secreted exosomes contain high levels of activated signaling proteins, such as phosphorylated Akt (T308), VEGFR2 (Y951) or PDGFRβ (Y751). Another protein that is highly enriched in exosomes is TLR3; Toll Like Receptors (TLRs) are important for innate immunity, recognizing highly conserved molecular patterns that are common to broad pathogen classes (Kawai and Akira, 2010). Cellular localization of TLRs has important consequences for ligand accessibility and downstream signaling events (Barton and Kagan, 2009); TLR3, as well as other TLRs involved in recognition of nucleic acids, is tipically located in endolysosomes. The finding here that exosomes contain high levels of TLR3 suggests a new possible way of action for TLR3, and might also have physiological and therapeutical implications for AMD. TLR3 has in fact been reported to be involved in sequence- and target-independent angiogenesis suppression (Kleinman et al, 2008; Cho et al, 2009) and retinal degeneration (Kleinman et al, 2012) induced by siRNAs in a mouse model of choroidal neovascularization. Furthermore, human choroidal neovascular membranes from AMD patients were shown to express TLR3 exclusively in RPE cells (Maloney et al, 2009); in view of the differences in RPE staining for TLR3 among samples, a possible role for this receptor in neovascular AMD was hypothesized.

Exposure of cells to oxidative stress induced in exosomes a change in the levels of various phosphorylated signaling proteins. Sets of these proteins are linked together in pathways regulating cell proliferation and survival (i.e., PDK1 (S241), Akt (T308), Elk1 (S383), ERK1/2 (T202/Y204), Src family (Y416)), cell death (i.e., Smac/Diablo, Bak), and cell metabolism (i.e., AMPK α1 (S485), Acetyl-CoA Carboxylase (S79), LDHA).

Our data suggests that exosomes do not simply reflect the average protein composition of the cell. The specific recruitment of proteins into exosomes is a matter of big interest, but it is still only partially understood. Among the factors involved in the sorting of cargo are specific interactions with lipids and proteins on membrane sub-domains, and interactions with tetraspanins (i.e., cd9, cd63); also the ESCRT complex, implicated in MVBs formation, is involved in selective cargo sorting (Fevrier and Raposo, 2004; Pant et al, 2012).

ROS, in particular H_2O_2, act as intracellular messengers; they can have a proliferative effect (Groeger et al, 2009) or, on the other hand, they can induce apoptosis (Circu and Aw, 2010) and, at higher levels, necrosis (Vanlangenakker et al, 2008). The final effect depends on the cellular context and on the quantitative and temporal aspects of ROS production (e.g. Gough and Cotter, 2011). In our case, a decreased activation of prosurvival pathways and an increase of some pro-apoptotic proteins were detected both in stressed cells and exosomes; however, the prooxidant treatment was not strong enough to induce a decrease in cell viability.

Exosomes from treated cells were found to contain a set of proteins that reflect a metabolic cell response to redox stress; ROS cause AMPK activation, which in turn phosphorylates and inactivates AcetylCoA Carboxylase (Ha et al, 1994) and up-regulates glycolytic enzymes such as lactate dehydrogenase (LDHA) (Wu and Wei, 2012).

It is known that exosomes can transfer functional proteins, miRNAs and mRNAs to recipient cells (Pant et al, 2012). Our finding that exosomes contain a large set of proteins in their phosphorylated form suggests that these vesicles have the potential to alter and/or regulate signaling cascades in recipient cells. Furthermore, exosomes may represent the way through which non-secreted (phospho)proteins are shed by retinal cells into the vitreous; they may thus constitute the route through which potential biomarkers reach easy-to-access body fluids, constituting candidate analytes for early diagnosis and/or personalized therapy. Despite the presence of the overlying neural retina, we hypothesize that exosomes secreted by RPE cells have the potential to reach the vitreous *in vivo*, thanks to their small size. This hypothesis is supported by *in vivo* data with nanoparticles, developed for slow-release drug delivery and/or gene delivery, and similar in size to exosomes (about 100-150 nm in diameter). It was reported that, after intra-vitreous injection, nanoparticles are able to migrate through the retinal layers and reach the RPE cells (Bejjani et al 2005; Birch and Qi Liang 2007; Bourges et al 2003). A retrograde flow (from RPE cells to the vitreous) is thus plausible.

Conclusions

ARPE-19 cells secrete through exosomes a great variety of signaling proteins, and the exosome content is perturbed by exposing ARPE-19 cells to oxidative stress under conditions that do not cause cell death.

RPMA permits the highly specific quantitation of post-translationally modified proteins, even when present at low abundance. Since phosphorylation reflects the activation state of signaling pathways, characterization of the phosphoprotein content may be critical for defining the role of exosomes in intercellular signaling.

13 proteins, 38 phosphoproteins and 3 cleaved proteins were detected in exosomes for the first time during this study; interestingly, many of these were also detected in the vitreous of patients with AMD (Davuluri et al, 2009; Espina et al, unpublished results). This strengthens the idea that these small vesicles may represent the way by which cells in the retina secrete intracellular/non soluble/receptor proteins into the vitreous. Detection of exosomes markers (cd-9, cd-63) in the vitreous would confirm this hypothesis.

Supplementary Material

Refer to Web version on PubMed Central for supplementary material.

Acknowledgments

This work was funded by the University of Padova, George Mason University and the grant 1R21EY018942-01 to LAL from NIH/NEI. We thank Prof. S. Garbisa and Dr. M. Zoratti for their support and interest and for useful discussions.

Abbreviations

AFM	Atomic Force Microscopy
AMD	Age-related Macular Degeneration

ESCRT	Endosomal Sorting Complex Required for Transport
FBS	Fetal Bovine Serum
MVB	Multi Vesicular Bodies
ROS	Reactive Oxygen Species
RPE	Retinal Pigment Epithelium
RPMA	Reverse Phase Protein Arrays
TLR	Toll Like Receptor

References

Ahmed K, Xiang J. Mechanisms of cellular communication through intercellular protein transfer. J Cell Mol Med. 2011; 15:1458–73. [PubMed: 20070437]

Alcazar O, Hawkridge AM, Collier TS, Cousins SW, Bhattacharya SK, Muddiman DC, Marin-Castano ME. Proteomics characterization of cell membrane blebs in human retinal pigment epithelium cells. Mol Cell Proteomics. 2009; 8:2201–11. [PubMed: 19567368]

Andersen CL, Jensen JL, Ørntoft TF. Normalization of real-time quantitative reverse transcription-PCR data: a model-based variance estimation approach to identify genes suited for normalization, applied to bladder and colon cancer data sets. Cancer Res. 2004; 64:5245–50. [PubMed: 15289330]

Barton GM, Kagan JC. A cell biological view of Toll-like receptor function: regulation through compartmentalization. Nat Rev Immunol. 2009; 9:535–42. [PubMed: 19556980]

Bejjani RA, BenEzra D, Cohen H, Rieger J, Andrieu C, Jeanny JC, Gollomb G, Behar-Cohen FF. Nanoparticles for gene delivery to retinal pigment epithelial cells. Mol Vis. 2005; 11:124–32. [PubMed: 15735602]

Belting M, Wittrup A. Nanotubes, exosomes, and nucleic acid-binding peptides provide novel mechanisms of intercellular communication in eukaryotic cells: implications in health and disease. J Cell Biol. 2008; 183:1187–91. [PubMed: 19103810]

Birch DG, Liang FQ. Age-related macular degeneration: a target for nanotechnology derived medicines. Int J Nanomedicine. 2007; 2:65–77. [PubMed: 17722514]

Boulton M, Dayhaw-Barker P. The role of the retinal pigment epithelium: topographical variation and ageing changes. Eye (Lond). 2001; 15:384–9. [PubMed: 11450762]

Bourges JL, Gautier SE, Delie F, Bejjani RA, Jeanny JC, Gurny R, BenEzra D, Behar-Cohen FF. Ocular drug delivery targeting the retina and retinal pigment epithelium using polylactide nanoparticles. Invest Ophthalmol Vis Sci. 2003; 44:3562–9. [PubMed: 12882808]

Charboneau L, Tory H, Chen T, Winters M, Petricoin EF, Liotta L, Paweletz C. Utility of reverse phase protein arrays: applications to signalling pathways and human body arrays. Brief Funct Genomic Proteomic. 2002; 1:305–15. [PubMed: 15239896]

Chiechi A, Mueller C, Boehm KM, Romano A, Benassi MS, Picci P, Liotta LA, Espina V. Improved data normalization methods for reverse phase protein microarray analysis of complex biological samples. Biotechniques. 2012; 0:1–7. [PubMed: 22946677]

Cho WG, Albuquerque RJ, Kleinman ME, Tarallo V, Greco A, Nozaki M, Green MG, Baffi JZ, Ambati BK, De Falco M, Alexander JS, Brunetti A, De Falco S, Ambati J. Small interfering RNA-induced TLR3 activation inhibits blood and lymphatic vessel growth. Proc Natl Acad Sci U S A. 2009; 106:7137–42. [PubMed: 19359485]

Circu ML, Aw TY. Reactive oxygen species, cellular redox systems, and apoptosis. Free Radic Biol Med. 2010; 48:749–62. [PubMed: 20045723]

Davuluri G, Espina V, Petricoin Er, Ross M, Deng J, Liotta L, Glaser B. Activated VEGF receptor shed into the vitreous in eyes with wet AMD: a new class of biomarkers in the vitreous with potential for predicting the treatment timing and monitoring response. Arch Ophthalmol. 2009; 127:613–21. [PubMed: 19433709]

Ding X, Patel M, Chan C. Molecular pathology of age-related macular degeneration. Prog Retin Eye Res. 2009; 28:1–18. [PubMed: 19026761]

Dorey C, Wu G, Ebenstein D, Garsd A, Weiter J. Cell loss in the aging retina. Relationship to lipofuscin accumulation and macular degeneration. Invest Ophthalmol Vis Sci. 1989; 30:1691–9. [PubMed: 2759786]

Dunn K, Aotaki-Keen A, Putkey F, Hjelmeland L. ARPE-19, a human retinal pigment epithelial cell line with differentiated properties. Exp Eye Res. 1996; 62:155–69. [PubMed: 8698076]

Février B, Raposo G. Exosomes: endosomal-derived vesicles shipping extracellular messages. Curr Opin Cell Biol. 2004; 16:415–21. [PubMed: 15261674]

Finnemann S. Focal adhesion kinase signaling promotes phagocytosis of integrin-bound photoreceptors. EMBO J. 2003; 22:4143–54. [PubMed: 12912913]

Gehrs K, Anderson D, Johnson L, Hageman G. Age-related macular degeneration-emerging pathogenetic and therapeutic concepts. Ann Med. 2006; 38:450–71. [PubMed: 17101537]

Gonzales PA, Pisitkun T, Hoffert JD, Tchapyjnikov D, Star RA, Kleta R, Wang NS, Knepper MA. Large-scale proteomics and phosphoproteomics of urinary exosomes. J Am Soc Nephrol. 2009; 20:363–79. [PubMed: 19056867]

Gough DR, Cotter TG. Hydrogen peroxide: a Jekyll and Hyde signalling molecule. Cell Death Dis. 2011; 2:e213. [PubMed: 21975295]

Groeger G, Quiney C, Cotter TG. Hydrogen peroxide as a cell-survival signaling molecule. Antioxid Redox Signal. 2009; 11:2655–71. [PubMed: 19558209]

Ha J, Daniel S, Broyles SS, Kim KH. Critical phosphorylation sites for acetyl-CoA carboxylase activity. J Biol Chem. 1994; 269:22162–8. [PubMed: 7915280]

Jager R, Mieler W, Miller J. Age-related macular degeneration. N Engl J Med. 2008; 358:2606–17. [PubMed: 18550876]

Johnson E. Age-related macular degeneration and antioxidant vitamins: recent findings. Curr Opin Clin Nutr Metab Care. 2010; 13:28–33. [PubMed: 19841580]

Kaarniranta K, Salminen A. Age-related macular degeneration: activation of innate immunity system via pattern recognition receptors. J Mol Med. 2009; 87:117–23. [PubMed: 19009282]

Kawai T, Akira S. The role of pattern-recognition receptors in innate immunity: update on Toll-like receptors. Nat Immunol. 2010; 11:373–84. [PubMed: 20404851]

Kevany B, Palczewski K. Phagocytosis of retinal rod and cone photoreceptors. Physiology (Bethesda). 2010; 25:8–15. [PubMed: 20134024]

Kleinman ME, Kaneko H, Cho WG, Dridi S, Fowler BJ, Blandford AD, Albuquerque RJ, Hirano Y, Terasaki H, Kondo M, Fujita T, Ambati BK, Tarallo V, Gelfand BD, Bogdanovich S, Baffi JZ, Ambati J. Short-interfering RNAs induce retinal degeneration via TLR3 and IRF3. Mol Ther. 2012; 20:101–8. [PubMed: 21988875]

Kleinman ME, Yamada K, Takeda A, Chandrasekaran V, Nozaki M, Baffi JZ, Albuquerque RJ, Yamasaki S, Itaya M, Pan Y, Appukuttan B, Gibbs D, Yang Z, Karikó K, Ambati BK, Wilgus TA, DiPietro LA, Sakurai E, Zhang K, Smith JR, Taylor EW, Ambati J. Sequence- and target-independent angiogenesis suppression by siRNA via TLR3. Nature. 2008; 452:591–7. [PubMed: 18368052]

Koopman W, Nijtmans L, Dieteren C, Roestenberg P, Valsecchi F, Smeitink J, Willems P. Mammalian mitochondrial complex I: biogenesis, regulation, and reactive oxygen species generation. Antioxid Redox Signal. 2010; 12:1431–70. [PubMed: 19803744]

Lu L, Hackett SF, Mincey A, Lai H, Campochiaro PA. Effects of different types of oxidative stress in RPE cells. J Cell Physiol. 2006; 206:119–25. [PubMed: 15965958]

Maa MC, Leu TH. Vanadate-dependent FAK activation is accomplished by the sustained FAK Tyr-576/577 phosphorylation. Biochem Biophys Res Commun. 1998; 251:344–9. [PubMed: 9790958]

Maloney SC, Antecka E, Orellana ME, Fernandes BF, Odashiro AN, Eghtedari M, Burnier MN Jr. Choroidal neovascular membranes express toll-like receptor 3. Ophthalmic Res. 2010; 44:237–41. [PubMed: 20699627]

Mathivanan S, Fahner CJ, Reid GE, Simpson RJ. ExoCarta 2012: database of exosomal proteins, RNA and lipids. Nucleic Acids Res. 2012; 40(Database issue):D1241–4. [PubMed: 21989406]

Mathivanan S, Simpson R. ExoCarta: A compendium of exosomal proteins and RNA. Proteomics. 2009; 9:4997–5000. [PubMed: 19810033]

Miceli M, Liles M, Newsome D. Evaluation of oxidative processes in human pigment epithelial cells associated with retinal outer segment phagocytosis. Exp Cell Res. 1994; 214:242–9. [PubMed: 8082727]

Mueller C, Liotta LA, Espina V. Reverse phase protein microarrays advance to use in clinical trials. Mol Oncol. 2010; 4:461–81. [PubMed: 20974554]

Nandrot E, Kim Y, Brodie S, Huang X, Sheppard D, Finnemann S. Loss of synchronized retinal phagocytosis and age-related blindness in mice lacking alphavbeta5 integrin. J Exp Med. 2004; 200:1539–45. [PubMed: 15596525]

Ng K, Gugiu B, Renganathan K, Davies M, Gu X, Crabb J, Kim S, Rózanowska M, Bonilha V, Rayborn M, Salomon R, Sparrow J, Boulton M, Hollyfield J, Crabb J. Retinal pigment epithelium lipofuscin proteomics. Mol Cell Proteomics. 2008; 7:1397–405. [PubMed: 18436525]

Oliver FJ, de la Rubia G, Rolli V, Ruiz-Ruiz MC, de Murcia G, Murcia JM. Importance of poly(ADP-ribose) polymerase and its cleavage in apoptosis. Lesson from an uncleavable mutant. J Biol Chem. 1998; 273:33533–9. [PubMed: 9837934]

Palanisamy V, Sharma S, Deshpande A, Zhou H, Gimzewski J, Wong D. Nanostructural and transcriptomic analyses of human saliva derived exosomes. PLoS One. 2010; 5:e8577. [PubMed: 20052414]

Palmisano G, Jensen SS, Le Bihan MC, Laine J, McGuire JN, Pociot F, Larsen MR. Characterization of membrane-shed micro-vesicles from cytokine-stimulated beta-cells using proteomics strategies. Mol Cell Proteomics. 2012; 11:230–43. [PubMed: 22345510]

Pant S, Hilton H, Burczynski ME. The multifaceted exosome: biogenesis, role in normal and aberrant cellular function, and frontiers for pharmacological and biomarker opportunities. Biochem Pharmacol. 2012; 83:1484–94. [PubMed: 22230477]

Plafker S. Oxidative stress and the ubiquitin proteolytic system in age-related macular degeneration. Adv Exp Med Biol. 2010; 664:447–56. [PubMed: 20238046]

Qin S. Oxidative damage of retinal pigment epithelial cells and age-related macular degeneration. Drug Develop Res. 2007; 68:213–225.

Schlaepfer DD, Hauck CR, Sieg DJ. Signaling through focal adhesion kinase. Prog Biophys Mol Biol. 1999; 71:435–478. [PubMed: 10354709]

Sharma S, Rasool H, Palanisamy V, Mathisen C, Schmidt M, Wong D, Gimzewski J. Structural-mechanical characterization of nanoparticle exosomes in human saliva, using correlative AFM, FESEM, and force spectroscopy. ACS Nano. 2010; 4:1921–6. [PubMed: 20218655]

Simpson R, Jensen S, Lim J. Proteomic profiling of exosomes: current perspectives. Proteomics. 2008; 8:4083–99. [PubMed: 18780348]

Speer R, Wulfkuhle J, Espina V, Aurajo R, Edmiston K, Liotta L, Petricoin EF. Development of reverse phase protein microarrays for clinical applications and patient-tailored therapy. Cancer Genomics Proteomics. 2007; 4:157–64. [PubMed: 17878519]

Suntres Z. Role of antioxidants in paraquat toxicity. Toxicology. 2002; 180:65–77. [PubMed: 12324200]

Tamburro D, Facchiano F, Petricoin EF, Liotta LA, Zhou W. Mass spectrometry-based characterization of the vitreous phosphoproteome. Proteomics Clin Appl. 2010; 4:839–46. [PubMed: 21137027]

Théry C, Amigorena S, Raposo G, Clayton A. Isolation and characterization of exosomes from cell culture supernatants and biological fluids. Curr Protoc Cell Biol. 2006 Chapter 3:Unit 3.22.

Théry C, Boussac M, Véron P, Ricciardi-Castagnoli P, Raposo G, Garin J, Amigorena S. Proteomic analysis of dendritic cell-derived exosomes: a secreted subcellular compartment distinct from apoptotic vesicles. J Immunol. 2001; 166:7309–18. [PubMed: 11390481]

Théry C, Zitvogel L, Amigorena S. Exosomes: composition, biogenesis and function. Nat Rev Immunol. 2002; 2:569–79. [PubMed: 12154376]

Tschopp J. Mitochondria: Sovereign of inflammation? Eur J Immunol. 2011; 41:1196–202. [PubMed: 21469137]

van Niel G, Porto-Carreiro I, Simoes S, Raposo G. Exosomes: a common pathway for a specialized function. J Biochem. 2006; 140:13–21. [PubMed: 16877764]

Vanlangenakker N, Vanden Berghe T, Krysko DV, Festjens N, Vandenabeele P. Molecular mechanisms and pathophysiology of necrotic cell death. Curr Mol Med. 2008; 8:207–20. [PubMed: 18473820]

VanMeter A, Rodriguez A, Bowman E, Jen J, Harris C, Deng J, Calvert V, Silvestri A, Fredolini C, Chandhoke V, Petricoin EF, Liotta L, Espina V. Laser capture microdissection and protein microarray analysis of human non-small cell lung cancer: differential epidermal growth factor receptor (EGPR) phosphorylation events associated with mutated EGFR compared with wild type. Mol Cell Proteomics. 2008; 7:1902–24. [PubMed: 18687633]

VanMeter A, Signore M, Pierobon M, Espina V, Liotta L, Petricoin EF. Reverse-phase protein microarrays: application to biomarker discovery and translational medicine. Expert Rev Mol Diagn. 2007; 7:625–33. [PubMed: 17892368]

Wang A, Lukas T, Yuan M, Du N, Tso M, Neufeld A. Autophagy and exosomes in the aged retinal pigment epithelium: possible relevance to drusen formation and age-related macular degeneration. PLoS One. 2009; 4:e4160. [PubMed: 19129916]

Weigel A, Handa J, Hjelmeland L. Microarray analysis of H2O2-, HNE-, or tBH-treated ARPE-19 cells. Free Radic Biol Med. 2002; 33:1419–32. [PubMed: 12419474]

Wilson B, Liotta L, Petricoin EF. Monitoring proteins and protein networks using reverse phase protein arrays. Dis Markers. 2010; 28:225–32. [PubMed: 20534907]

Wolf G. Lipofuscin and macular degeneration. Nutr Rev. 2003; 61:342–6. [PubMed: 14604266]

Wu SB, Wei YH. AMPK-mediated increase of glycolysis as an adaptive response to oxidative stress in human cells: implication of the cell survival in mitochondrial diseases. Biochim Biophys Acta. 2012; 1822:233–47. [PubMed: 22001850]

Wu Y, Yanase E, Feng X, Siegel M, Sparrow J. Structural characterization of bisretinoid A2E photocleavage products and implications for age-related macular degeneration. Proc Natl Acad Sci U S A. 2010; 107:7275–80. [PubMed: 20368460]

Yu D, Cringle S. Oxygen distribution and consumption within the retina in vascularised and avascular retinas and in animal models of retinal disease. Prog Retin Eye Res. 2001; 20:175–208. [PubMed: 11173251]

Zarbin M. Current concepts in the pathogenesis of age-related macular degeneration. Arch Ophthalmol. 2004; 122:598–614. [PubMed: 15078679]

Highlights

- ARPE-19 cells secrete through exosomes a great variety of signaling proteins
- Reverse Phase Protein Arrays technology was used to characterize exosome content
- 72 proteins were detected in exosomes, 41 in post-translationally modified form
- Exosome content is perturbed by exposing ARPE-19 cells to oxidative stress
- Phosphoprotein content may be critical for the signaling role of exosomes

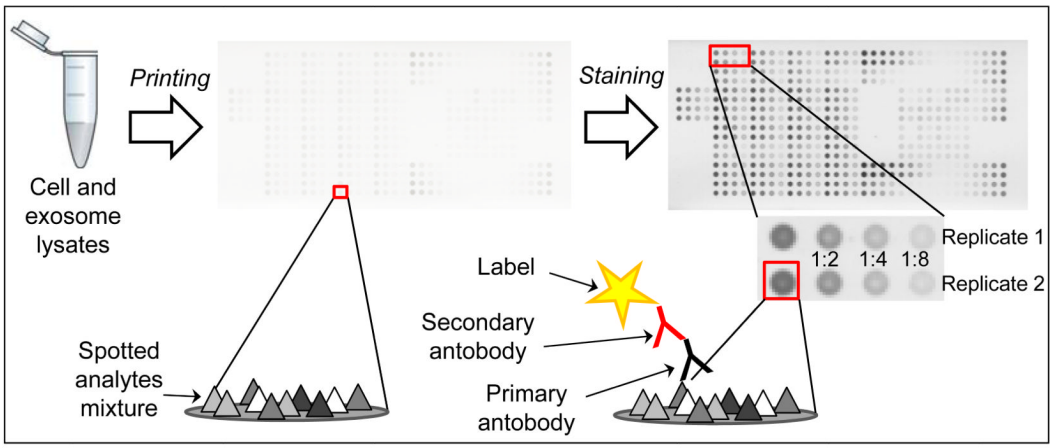

Fig. 1. RPMA technology

Sample lysates and controls are immobilized on a nitrocellulose-coated slide and probed with a primary and secondary antibody. The signal is amplified via horseradish peroxidase-mediated deposition of biotinyl tyramide. Cell lysates are prepared in a 2-fold dilution series, allowing analysis within the linear dynamic range for each sample-antibody pair.

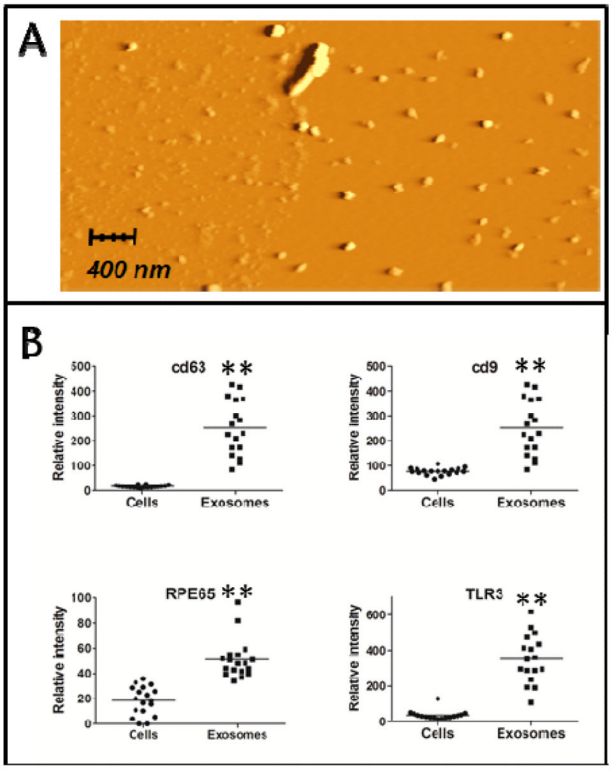

Fig. 2. Exosome characterization

A: AFM image of exosomes isolated after a 24h treatment with Methyl Viologen. B: cd9, cd63, RPE-65 and TLR3 protein levels in ARPE-19 cells and exosomes (N = 18). **: significantly different from the cell lysates (Mann-Whitney test, $p \leq 0{,}001$).

Protein	Treatment		Accession number		Kegg Pathway #
	Rotenone	Methyl Viologen	Uniprot	Kegg	A
Downregulated					
Akt (T308)	x	x	P31749	K04456	4010,4012,4062,4150,4210,4370,4510,4530,4620,4630,4722,4910,4920,4973
Bad (S155)		x	Q92934	K02158	4012,4210,4370,4510,4722,4910
cKit (Y703)	x	96h	P10721	K05091	4060,4144
cKit (Y719)		x	P10721	K05091	4060,4144
Cl. Casp7 (D198)		x	P55210	K04397	4210
Cofilin	x	x	P23528	K05765	4810
cRaf (S338)	x	x	P04049	K04366	4010,4012,4062,4370,4510,4540,4650,4722,4810,4910
eIF4G (S1108)	x		Q04637	K03260	3013
eNOS (S1177)	x	x	P29474	K13242	330,402
eNOS/NOS III (S116)	x	x	P29474	K13242	330,402
ERK (T202/Y204)	x		P28482,P27361	K04371	4010,4012,4062,4150,4350,4370,4510,4520,4540,4620,4621,4650,4722,4810,4910
FAK (Y576/577)	x	x	Q05397	K05725	4012,4062,4370, 4510,4810,5100
FAK (Y397)	x	x	Q05397	K05725	4012,4062,4370,4510,4810,5100
GSK3$_{\alpha\beta}$ (Y279/Y216)	x	x	P49840	K08822,K03083	4012,4062,4110,4310,4340,4510,4722,4910
HO-1	x	x	P09601	K00510	860,4978
Hsp27	x		P04792	K09543	5169
IRS1 (S612)	x		P35568	K07187	4722,4910,4920
p38	x	x	Q16539	K04441	4010,4370,4620,4621,4622,4722
p38 (T180/Y182)	x		Q16539	K04441	4010,4370,4620,4621,4622,4722
PDGFR$_{\beta}$ (Y716)	x	x	P16234	K05089	4010,4020,4060,4510,4540,4810
PDGFR$_{\beta}$ (Y751)	x	x	P16234	K05089	4010,4020,4060,4510,4540,4810
PDK1 (S241)	x		O15530	K06276	3320,4150,4510,4910
PTEN (S380)	x		P60484	K01110	562,4070,4115,4510,4530
RPE-65		x	Q16518	K11158	830
S6 (S240/244)	x	24h	P62753	K02990	3010
SHIP1 (S727)	x		Q92835	K03084	562,407
Src (Y416)	x		P12931	K05704	4012,4062,4144,4370,4510,4520,4530,4540,4810,5100
Stat5 (Y694)	x		P42229,P51692	K11223,K11224	4012,4630,5200,4062
TLR3	x	x	O15455	K05401	4620
TLR9		x	Q9NR96	K10161	4620
Tyk2 (Y1054)	x	x	P29597	K11219	4630
VEGFR2 (Y996)	x	x	P35968	K05098	4060,4144,4370,4510
Upregulated					
AcetylCoA carb (S79)	x		O00763	K11262	61,620,640,4910
Apaf-1		x	O14727	K02084	4115,421
Atg5		x	Q9H1Y0	K08339	4140,4622
Atg12		x	O94817	K08336	4140,4622
Bad (S112)	x	x	Q92934	K02158	4012,4210,4370,4510,4722,4910
Beclin1		x	Q14457	K08334	4140
Biliverdin Reductase A		x	P53004	K00214	860
cKit (Y703)		24h	P10721	K05091	4060,4144
Cl. Casp3 (D175)	x	x	P42574	K02187	4010,4115,4210
Cl. Casp9 (D330)		x	P55211	K04399	4115,4210,4370
COX2	x		P35354	K11987	590,4064,4370
CREB (S133)	x	x	P16220	K05870	4612
iNOS	x	x	P35228	K13241	330,4020,4146
p90RSK (S380)		x	Q15418	K04373	4010, 4150,4722
PTEN (S380)		x	P60484	K01110	562,4070,4115,4510,4530
S6 (S240/244)		96h	P62753	K02990	3010
Stat3 (S727)	x	x	P40763	K04692	4062,4630,4920
Shc (Y317)		x	P29353	K06279	4012,4062,4510,4722,4910
VEGFR2 (Y951)		x	P35968	K05098	4060, 4144, 4370, 4510

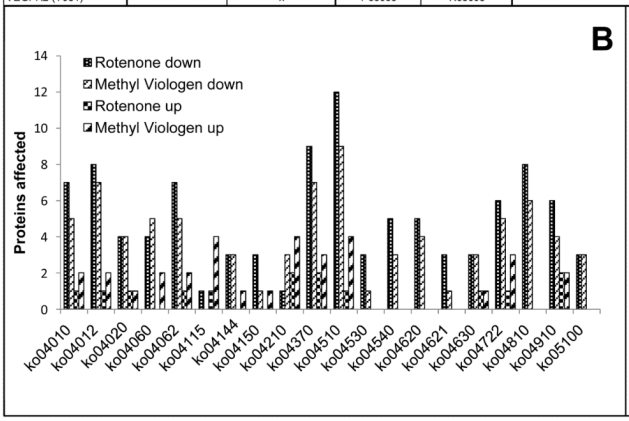

C

Kegg #	Pathway
ko04010	MAPK signaling pathway
ko04012	ErbB signaling pathway
ko04020	Calcium signaling pathway
ko04060	Cytokine-cytokine receptor interaction
ko04062	Chemokine signaling pathway
ko04115	p53 signaling pathway
ko04144	Endocytosis
ko04150	mTOR signaling pathway
ko04210	Apoptosis
ko04370	VEGF signaling pathway
ko04510	Focal adhesion
ko04530	Tight junction
ko04540	Gap junction
ko04620	Toll-like receptor signaling pathway
ko04621	NOD-like receptor signaling pathway
ko04630	Jak-STAT signaling pathway
ko04722	Neurotrophin signaling pathway
ko04810	Regulation of actin cytoskeleton
ko04910	Insulin signaling pathway
ko05100	Bacterial invasion of epithelial cells

Fig. 3. Down- and upregulated proteins in ARPE-19 cells after Rotenone or Methyl Viologen treatment

Down- or up-regulated signaling proteins in treated ARPE-19 cells, compared to control (Mann-Whitney test, $p \leq 0.1$). A. List of affected proteins; B. Proteins grouped in signaling pathways; C. Pathway description.

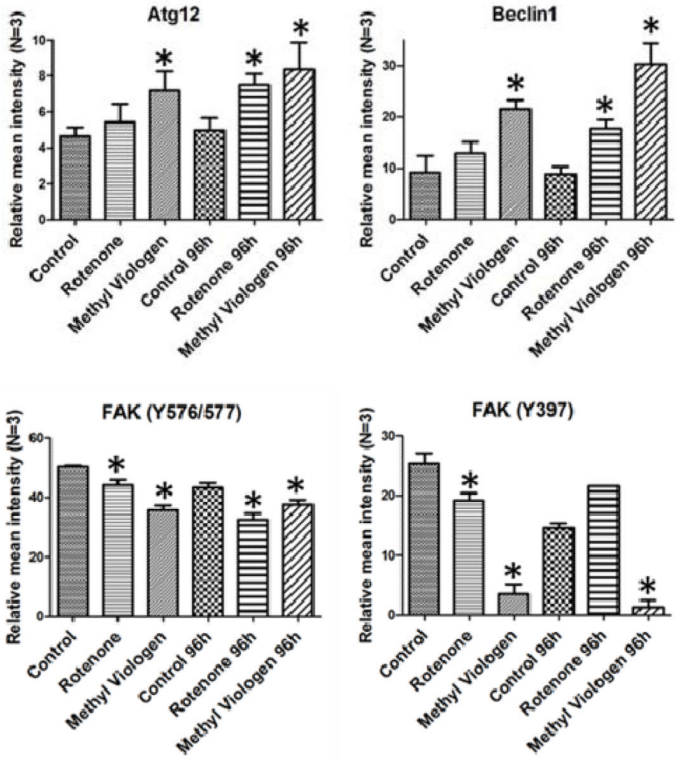

Fig. 4. Proteins altered in stressed ARPE-19 cells

Protein levels (Relative mean intensity ± SEM) in ARPE-19 cells treated with Rotenone or Methyl Viologen. *: significantly different from the corresponding control lysates (Mann-Whitney test, N=3, $p \leq 0,1$).

Tab. 1

Proteins detected in ARPE-19 exosomes and their relative abundance compared to cells

Abundance of proteins found in exosomes is expressed as higher (+), lower (−) or non-significantly different (ns) compared to ARPE-19 cell lysates. Anti-phosphoprotein antibodies are expressed with the name of the protein followed by the position of phosphorylation; for caspases, the cleavage position is indicated.

UniProt accession number	Protein	Previous detection in exosomes (Exocarta database)	Relative abundance
O00763	Acetyl-CoA Carboxylase (S79)	only total protein	ns
Q9UE89	β actin	yes	– *
P31749	Akt (T308)	only total protein	+ **
Q13131	$AMPK_{\alpha}1$ (S485)	only total protein	ns
Q9Y478	AMPKβ1 (S108)	no	ns
P07355	Annexin II	yes	ns
O14727	Apaf-1	yes	+ **
Q9H1Y0	Atg5	yes	– **
O94817	Atg12	yes	+ *
Q92934	Bad (S112)	no	+ *
Q92934	Bad (S155)	no	ns
Q16611	Bak	no	ns
Q07812	Bax	yes	– **
P10415	Bcl-2 (T56)	no	+ **
Q07817	Bcl-xL	no	
Q14457	Beclin-1	no	ns
P53004	Biliverdin Reductase	yes	+ **
P42574	Caspase-3, cleaved (D175)	no	ns
P55210	Caspase-7, cleaved (D198)	no	+ **
P55211	Caspase-9, cleaved (D330)	only total protein	+ *
P21926	cd9	yes	+ **
P08962	cd63	yes	+ **
P10721	c-Kit (Y703)	no	ns
P10721	c-Kit (Y719)	no	ns
P23528	Cofilin	yes	ns
P35354	Cox-2	no	+ **
P04049	c-Raf (S338)	no	ns
P16220	CREB (S133)	no	ns
P13073	Cytochrome c oxidase- Complex IV, Sub. IV	yes	ns
P10606	Cytochrome c oxidase- Complex IV, Sub.Vb	yes	ns
Q04637	eIF4G (S1108)	only total protein	– **

UniProt accession number	Protein	Previous detection in exosomes (Exocarta database)	Relative abundance
P19419	Elk-1 (S383)	no	ns
P29474	eNOS (S1177)	no	– *
P29474	eNOS/NOS III (S116)	no	ns
P28482, P27361	ERK 1/2 (T202/Y204)	only total protein	– **
Q05397	FAK (Y397)	no	ns
Q05397	FAK (Y576/577)	no	ns
P49840	GSK-3αβ (Y279/Y216)	no	ns
P09601	Heme-Oxygenase-1	no	– **
P04792	HSP27 Protein 1	yes	– *
P07900	HSP90	yes	
P35228	i-NOS	no	ns
P35568	IRS-1 (S612)	only total protein	– *
P13473	LAMP-2	yes	ns
Q9GZQ8	LC3B	yes	ns
P00338	LDHA	yes	– **
Q6LEN1	Mn Superoxide Dismutase	yes	+ *
P42345	mTOR (S2481)	no	– **
Q16539	p38 MAP Kinase	no	– *
Q16539	p38 MAP Kinase (T180/Y182)	no	ns
Q9GZT9	PHD-2/Egln1	no	– **
P19838	NF-kappaB	no	
P19838	NF-kappaB p65 (S536)	no	+ **
Q15418	p90RSK (S380)	only total protein	ns
P16234	PDGFRβ (Y716)	only total protein	+ **
P16234	PDGFRβ (Y751)	only total protein	ns
O15530	PDK1 (S241)	no	– *
P60484	PTEN (S380)	no	– **
Q16518	RPE65	no	+ **
P62753	S6 Ribosomal Protein (S240/244)	only total protein	– *
P45983	SAPK/JNK (T183/Y185)	only total protein	– *
P29353	Shc (Y317)	no	+ *
Q92835	SHIP1 (Y1020)	no	ns
Q9NR28	Smac/Diablo	no	– **
P12931	Src Family (Y416)	only total protein	– *
P40763	Stat3 (S727)	no	ns

UniProt accession number	Protein	Previous detection in exosomes (Exocarta database)	Relative abundance
P42229, P51692	Stat5 (Y694)	no	– **
O15455	TLR3	no	+ **
Q9NR96	TLR9	no	+ **
P29597	Tyk2 (Y1054/1055)	only total protein	ns
P35968	VEGFR 2 (Y951)	no	+ **
P35968	VEGFR 2 (Y996)	no	– *

* significantly different from cell lysates (Mann-Whitney test, N=18; $p \leq 0{,}05$).

** significantly different from cell lysates (Mann-Whitney test, N=18; $p \leq 0{,}001$).

Tab. 2

Down- and upregulated proteins in ARPE-19 exosomes after Rotenone or Methyl Viologen treatment

List of the down- and up-regulated signaling proteins in exosomes shed by treated ARPE-19 cells, compared to control (Mann-Whitney test, $p \leq 0.1$).

Protein	UniProt accession number	Kegg accession number	Kegg Pathway #	same change correspondi cells
Downregulated				
Akt (T308)	P31749	K04456	4010,4012,4062,4150,4210,4370,4510,4530,4620,4630,4722,4910,4920,4973	x
Apaf-1	O14727	K02084	4115,421	
Atg5	Q9H1Y0	K08339	4140,4622	
Elk-1 (S383)	P19419	K04375	4010,4012,4510,4910	
ERK 1/2 (T202/Y204)	P28482, P27361	K04371	4010,4012,4062,4150,4350,4370,4510,4520,4540,4620,4621,4650,4722,4810,4910	x
p38 MAP Kinase (T180/Y182)	Q16539	K04441	4010,4370,4620,4621, 4622,4722	x
PDK1 (S241)	O15530	K06276	3320,4150,4510,4910	x
Src Family (Y416)	P12931	K05704	4012,4062,4144,4370,4510,4520,4530,4540,4810,5100	x
TLR9	Q9NR96	K10161	4620	x
Upregulated				
Acetyl-CoA Carboxylase (S79)	O00763	K11262	61,620,640,4910	x
$AMPK_{\alpha}1$ (S485)	Q13131	K07198	4140, 4150, 4910, 4920	
Bak	Q16611	K14021	4141	
LDHA	P00338	K03778	620	
Smac/Diablo	Q9NR28	K10522	4210	